Phase Correction of Emission Line Fourier Transform Spectra

Richard C. M. Learner and Anne P. Thorne
Blackett Laboratory, Imperial College
Prince Consort Road, London, SW7 2BZ, England

James W. Brault
National Solar Observatory
P.O. Box 26732, Tucson, Az, 85726, U.S.A.

Mark C. Abrams
Jet Propulsion Laboratory
California Institute of Technology
4800 Oak Grove Dr., Pasadena, Ca., 91109

Abstract

The process of phase correction for "emission line spectra with high signal-to-noise ratios has remained an unresolved problem and critically defines the quality and reproducibility of the Fourier transform emission spectra. Traditional methods utilize a low resolution phase spectrum and often produce spectra that do not have reproducible line positions. A phase correction strategy has been developed for and tested with infrared, visible, and UV emission line sources. A high resolution (64-80 K point interferogram) phase spectrum provides the phase data. A discriminator is used to restrict the phase data to those points that have sufficient signal-to-noise to obtain a reliable phase estimate, and a smooth phase function is obtained by fitting a polynomial to the phase data. Quantitative estimates of the phase error as a function of apodisation width, discriminator value, and order of polynomial used in the fitting process arc presented.

L Introduction

A spectrum can be exactly reconstructed from an ideal, symmetric interferogram by means of the cosine Fourier transform alone. In practice, sampled interferograms arc never entirely symmetric, and complete reconstruction requires a complex Fourier transform. The required real spectrum is recovered from the complex spectrum either by applying a phase correction or by taking the modulus, and it will be shown later that the first of these alternatives is preferable.

Asymmetry in the rccordcd interferogram may arise from a combination of several effects. First, neither the apodising function (including the truncation of the interferogram) nor the signal intensity arc necessarily symmetric about zero path difference. Second, the centre of the zero path fringe of a symmetrically apodised interferogram may not (and usually does not) coincide exactly with one of the points at which the interferogram is sampled. Third, any dispersive effects will make the optical path difference frequency dependent so that there is no well defined position of zero path difference. Such dispersive effects maybe optical - small differences in the beamsplitter and compensator thickness, for example - or electrical - frequency dependent delays in the amplifying and filtering electronics. When dispersion is present the brightest fringe, sometimes called the 'grand maximum', is taken as the centre, but the interferogram is not symmetric about this point.

The effect of an asymmetric apodising function $T(x)$ is to convolve the transformed spectrum with a complex instrument function $t(\sigma)$, where

$$t(\sigma) = \text{t,(o)} + it_a(\sigma). \tag{1}$$

Since $T(x)$ is - at least in principle - under the control of the operator, we start by taking it to be symmetric (i.e. $t_a(\sigma) = \text{O}$). The other two effects arc taken into account by writing the modulated part of the interferogram as

$$I(x) = \int_J A(\sigma)\cos[2\pi\sigma(x-\epsilon) - \text{t}\ \psi(\sigma)]d\sigma \tag{2}$$

where $A(\sigma)$ *is* the source distribution, c is the offset of the sampling grid, and $\psi(\sigma)$ is the dispersive phase. If the latter is the result of an refractive optical path mismatch δ it takes the form $\psi(\sigma) = 2\pi\sigma[n(\sigma)-1]6$, where n is the refractive index of the beamsplitter material. In general onc assumes that the functional form of ψ is not well known. The linear term $2\pi\sigma\epsilon$ can be incorporated with ψ to give

$$I(x) = \int_J A(\sigma)\cos[2\pi\sigma x - \text{t}\ \phi(\sigma)]d\sigma \tag{3}$$

where $\phi(\sigma) = 2\pi\sigma\epsilon + \psi(\sigma)$.

The complex Fourier transform of this function is

$$S(\sigma) = e^{-i\phi(\sigma)}A(\sigma). \tag{4}$$

To recover the true spectrum *A(u)* from the observed spectrum $S(\sigma)$, wc need to determine $\phi(\sigma)$ experimentally and multiply through by $e^{+i\phi(\sigma)}$: this is the process known as phase correction. If the

interferometer is to be used at or near its limit as a signal handling device (i.e., to give results limited in quality only by source or detector noise), the phase correction must be determined with a precision that greatly exceeds its day-to-day reproducibility. Phase correction must therefore be done-separately for each observed interferogram (or co-added set) and must be deduced from the data contained within the interferogram. When the effects of asymmetric apodisation are considered, it will be seen that a 'single-sided' interferogram is much more sensitive to errors in phase correction that is a 'double-sided' interferogram.

IL Basic approach to phase correction

a. Symmetric apodisation function

The phase $\phi(\sigma)$ is always a slowly varying function of the wavenumber σ, and the usual approach is to determine *tan* ϕ from the ratio of the imaginary and real parts of the complex spectrum obtained from a short section of the interferogram truncated symmetrically about the centre.

Intensity and resolution criteria have also been analysed by Brault [1] for both absorption and emission spectra. This distinction has relevance to the phase problem in two ways. The first is straightforward: in an absorption spectrum there is information at all frequencies, whereas in an emission spectrum there is information only at some frequencies, and that information can vary widely in quality. We arc concerned here with a pure emission line spectrum - that is, onc where the energy is concentrated entirely into the discrete lines. In this case the output of the transform in the gaps between the lines is incoherent white noise in both the real and imaginary parts, both parts having the same root mean square amplitude. The phase is undetermined: the mean value is arbitrary, and the RMS deviation from that mean is $\pm\pi/\sqrt{3}$ radians. Most of the spectral points contribute nothing to the phase data. The phase is determined only at each line, and then only to a precision set by the signal to noise ratio for that linc.

This problcm cannot bc overcomc by adding a weak continuous spectrum to the input. The photon noise associated with the total energy involved (individual channel energy times the very large number of channels) degrades the entire spectrum and is not acceptable. Using the modulus of thc spectrum (equivalent to ignoring phase correction) also degrades the signal to noise ratio.

In thc case of an emission spectrum relatively fcw spectral points carry useful phase information and an additional decision is required: the choice of the intensity below which phase information is not significant. The choice of resolution is also of much greater significance.

The aim is to achievc a phase correction such that residual errors of phase degrade the spectrum by an amount small compared with the noise. In some cases this can require the phase to bc determincd with an error of the order of magnitude (in radians) of the reciprocal of the signal to noise ratio in the computed spectrum -e.g. if the latter is 1000, the phase error should bc less than ± 1 mrad.

Wc need to consider first the errors $\delta(\sigma)$ in the phase found from the truncated section and second the effect on the final spectrum of phase correction with the function 4(o)+ $\delta(\sigma)$. Brault [1] has shown that for an emission linc at σ_0, the phase error is given by

$$tan[\delta(\sigma)] \approx \phi'(\sigma) \cdot (\sigma - \sigma_0) \approx \phi(\sigma) - \phi(\sigma_0) \qquad (5)$$

where $\phi'(\sigma) = \partial\phi(\sigma)/\partial\sigma$ is the gradient of the phase at σ_0. $\delta(\sigma)$ is proportional to the rate of change of the phase spectrum with frequency, if the truncation is short enough for the width of the instrument function to exceed that of the emission line. This phase error is equal to the phase change across the width of the instrument function, so that the phase is artificially flattened within a region of significant width. Evidently ϕ' can bc minimized by shifting the origin to make the linear phase term equal to zero in the spectral region of interest, regardless of whether this linear term comes from the grid displacement ϵ or from a linear term in the dispersive component. This is equivalent to choosing the origin to bc the point of *stationary phase* (to first order).

To get good phase data from emission spectra requires therefore that some discriminator (or highly nonlinear weighting function) be used to eliminate thc sea of phase noise lying between the lines.

The resulting phase data is a set of point values at arbitrary values of σ, and some smoothing process is required to link these to form an analytic function to be used for phase correction. The choice of function is not critical; the optimum in terms of minimizing the number of parameters would be onc that reflected the wave number dependance of the dispersive character of the components. In practice wc have used a polynomial, as discussed in Section 111.

The second problem for emission spectra is more subtle and more of a nuisance. It concerns the length of the symmetrically truncated central section of the interferogram used to determinc the phase function. As the length of this section decreases, thc instrument profile in the Fourier transform broadens. This is not of great significance in absorption spectra where the rate of change of intensity with frequency is small. In emission spectra the intensity variation between lines may bc as great as 10000:1. Under these conditions the wing of an instrumentally broadened line profile may overwhelm the peak of a weak line at another frequency. The phase information from the weak line will thus bc replaced by data for a line at a different frequency, Examples are given in Section 3 that illustrate the necessity of choosing the instrumental width in the *low resolution* spectrum to bc very much smaller than the typical interval between strong lines.

This need for a narrow instrumental width - that is for a fairly high *low resolution* apodisation - means that the functions of phase determination and phase smoothing must bc separate, A broad instrument function cannot bc used to smooth the phase data of an emission line spectrum.

b. Asymmetric apodisation function

The two extremes of apodisation arc nearly symmetric truncation (equal-sided interferograms) and almost completely asymmetric truncation (unequal-sided interferograms or, in the limit; one-sided

interferograms). The advantage of the latter is that it offers the maximum resolution for a given observation time, but, as shown below, it imposes more severe restrictions on the accuracy to which $\phi(\sigma)$ must be determined.

Truncation by an asymmetric function $T(x)$ leads to a complex instrument function with a large imaginary part, which is necessarily antisymmetric. Suppose the interferogram is observed from $-l$ to $+L$ $(l<L)$, and the portion from -1 to+/ is weighted onc half with respect to that from $+l$ to $+L$ as illustrated in Figure 1. Then the real part of the instrument function is the well-known sine function

$$t_s(\sigma) = L\,sinc(2\pi\sigma L) = L\frac{sin(2\pi\sigma L)}{2\pi\sigma L} \tag{6}$$

and the imaginary part is the antisymmetric cosine function

$$t_a(\sigma) = L\,cosinc(2\pi\sigma L) - l\,cosinc(2\pi\sigma l); \tag{7}$$

where in, analogy with the sine function,

$$cosinc(2\pi\sigma L) = cos(2\pi\sigma L)/(2\pi\sigma L). \tag{8}$$

If the interferogram is nearly one-sided with 1<<1. then,

$$t_a(\sigma) \rightarrow L\,cosinc(2\pi\sigma L) - \frac{1}{2\pi\sigma} = \frac{cos(2\pi\sigma L)-1}{2\pi\sigma} \tag{9}$$

Figure 2 illustrates symmetric and antisymmetric components of the apodisation function for an unequal-sided interferogram, and the complex instrument function in both the spatial and frequency domains. Multiplication of the interferogram by the asymmetric truncation function $T(x)$ leads to a convolution of the spectrum with this complex instrument function

$$T(x)I(x) \overset{DFT}{\Longleftrightarrow} [t,(u) + - \; it_a(\sigma)] * S(\sigma). \tag{lo}$$

If $S(\sigma)$ is wholly real (either because $I(x)$ is completely symmetric or because the phase correction is perfect), the real part of the convolution $t_s(\sigma) * S(\sigma)$ gives the required spectrum and the imaginary part can simply be discarded. The problem arises when the spectrum is imperfectly phase corrected, For a small residual phase error $\delta(\sigma)$,

$$S(u) = A(\sigma)e^{-i\delta(\sigma)} = A(\sigma)\,cos\,\delta - iA(\sigma)\,sin\,\delta \simeq A(\sigma) - i\delta A(\sigma). \tag{11}$$

The real part of the convolut ion now contains two parts: the real parl of the spectrum convolved with the symmetric part of the instrument function, and a second term which is the convolution of the imaginary part of the spectrum with the antisymmetric instrumental profile $t_a(\sigma)$:

$$Re[S(\sigma) * t(\sigma)] = A(a) * t,(o) + [6A(o)] * t_a(\sigma) \tag{12}$$

where $t_a(\sigma)$ is not small compared with $t_s(\sigma)$. If δ is small and effectively constant over the instrument profile, it can be taken out of the convolution to give

$$Re[S(\sigma) * t(\sigma)] = A(\sigma) * [t_s(\sigma) + \delta(\sigma) t_a(\sigma)]. \quad (13)$$

This asymmetric instrument function displaces and distorts all observed lines by an amount proportional to the local phase error. For $1 \approx O$ and an unresolved line (sine profile) the wavenumber error is 0.56 times the resolution element and Brault has evaluated an equivalent shift for Lorentzian and Gaussian line profiles of 0.50δ and 0.486 respectively.

In the intermediate case, $O < l < L$, the relative amplitude of the antisymmetric part of the instrument function is of course reduced, but not in proportion to the *double-sidedness.* For a 4:1 asymmetry ($l = L/4$) the reduction in wavenumber shift for a given phase error is only 8%. In a double-sided interferogram the antisymmetric part of the interferogram approaches zero, and the sensitivity to phase error is minimal. Phase correction in the equal-sided case gives, in effect, a $\sqrt{2}$ gain in signal to noise ratio. Thus, the procedure for determining the phase outlined at the beginning of this section uses a symmetrically truncated central section of the interferogram to avoid distortion from an asymmetric instrument function.

III. Experimental data

A phase correction strategy derived from the previous paragraphs was developed for and tested with infrared, visible, and UV emission line sources. The spectra considered here are dominantly those of the Iron-Argon or Iron-Neon hollow cathode and were taken to underpin a reobservation of the Fe I spectrum. A brief summary of the Fourier transform spectrometer, the light source, and the observed spectra is therefore relevant.

The FTS at the National Solar Observatory - Tucson, Az. is a one metre Connes type Michelson interferometer with complementary inputs and outputs.

Typical parameters for an observing run at NSO were: a one million point interferogram at a resolution of 800000 (i.e., 4:1 asymmetry) consisting of 10 to 20 co-added scans in a one to two hour observation time. The spectral ranges were restricted by optical and electrical filters to about 10000 cm^{-1} in an overall coverage from 1850 to 35000 cm^{-1}, Observations were principally in first order alias, though occasionally second or third order aliases were used: in all cases the highest frequency observed was usually at about 0.9 times the frequency of the alias edge. Several different types of diode detectors (Si, UV Si, InSb) were used, as appropriate. Electrical filtering was by analogue means (the phase shifts of these filters were the dominant contributor to the overall phase error [1]) and the data was digitally recorded.

The light sources were high current hollow cathode lamps, usually run in Neon or Argon. Typically filling pressures were 4 Torr (Neon) and 3 Torr (Argon), and the current was usually between 0.75 and one ampere. The majority of the observations were made with an uncooled pure iron cathode.

Continuum radiation from the red-hot cathode was excluded by careful focusing and by using a tilted rear window to the lamp to avoid unwanted reflections. Such radiation can easily dominate the photon noise in the red and infrared spectral regions which sets the fundamental limit on the quality of the observations.

IIIa. Spectra and wavenumber calibration

The resulting spectra contain a large number of lines with widths corresponding to a Doppler temperature around 2450 K (a line with FWHM of 0.100 cm^{-1} at 22000 cm^{-1}). The resolution step was chosen to give about four points in this line width. Typical low resolution amplitude and phase spectra arc given in Figure 3. The phase spectrum is well defined in the regions where the signal to noise ratio is large; however, as the signal to noise ratio decreases, the phase spectrum becomes increasingly noisy. Initially the spectra were phase corrected using a low resolution phase spectrum determined from a transform of 4096 points centred about the central fringe of the interferogram. Overlapping spectra were taken to obtain continuous high resolution coverage of the spectrum with high signal to noise ratio. After the line positions were measured, wavenumbers of overlapping regimes of different runs were compared.

In most cases pairs of FTS spectra did not give reproducible line wavenumbers, as the wavenumber differences in Figure 4 demonstrate: the scatter of the differences at either end of the wavenumber region suggests that there is no dispersion between the spectra, but the systematic wavenumber error for lines between 20000 and 24000 cm^{-1} suggests that the line shapes in onc of the spectra are distorted sufficiently to produce the wavenumber shifts observed. Line shape distortion can occur in asymmetric interferograms if the phase is corrected improperly. A comparison with Figure 3 indicates that the lines in this spectral region arc relatively weak compared to lines below 20000 and above 24000 cm^{-1} .

IVa. High resolution phase determination

The traditional method for determining the phase uses a transform of 4096 points of the interferogram centered about the grand maximum to generate a low resolution phase with which the high resolution complex spectrum can bc rotated into a real, phase corrected, spectrum. In such a process, the apodisation and thc phase smoothing arc accomplished simultaneously. Presuming that the wavenumber difference.. presented in Figure 3 resulted from inadequate phase correction, an alternate method was suggested in which the phase apodisation and phase smoothing were performed separately. The low resolution phase correction was performed as follows:

- the interferogram was apod ised to obtain a two-sided interferogram (4192-81920 points in length)
- the phase spectrum was determined from the transform for all data points exceeding a specified discriminator. This insures that the phase will bc determined only from points with sufficient amplitude to yield a reliable phase estimate.
- the phase spectrum was smoothed by fitting the spectrum to a polynomial with 3-8 terms.

• the high resolution spectrum was phase corrected with the polynomial representation of the phase.

Pairs of spectra were then compared to check the reproducibility of wavenumbers in overlapping regions.

IVb. Apodization

While the phase of a spectrum is assumed to be a slowly varying function of wavenumber, the resolution width used in the phase determination averages a certain number of data points to obtain the phase estimate. In a case such as the spectrum presented in Figure 3a, a low resolution phase estimate allows the phase of the strong lines below 20000 cm^{-1} and above 24000 cm^{-1} to propagate into the intermediate region where the phase is significantly different but there arc no strong lines, In all cases a cosine bell apodisation function given by the expression

$$T(x) = \left[\frac{1}{2}(1 + cos(\theta)\right]^{\pi}_{1-\pi} \tag{14}$$

was used. Figure 5 presents phase differences between a phase estimate using 81920 points and lower resolution runs with 40960, 204S0, and 4096 samples. The phase differences arc minimal for the high resolution phase determination and accurate estimation of the phase in the region between 20000 and 24000 cm^{-1} (where the signal to noise ratio is considerably smaller than elsewhere) requires more than 40000 points. The phase error as a function of apodisation width is displayed in Figure 6, which indicates that phase errors at the milliradian level require an apodisation width of 40000 points or more.

IVc. Discriminator

The goal of phase correction is to produce a spectrum in which the error in line position determination is dominated by noise rather than computational artifacts. For a nearly symmetric interferogram ($l \approx$ O) the condition that

$$\delta\sigma_{phase} < \delta\sigma_{noise}$$

corresponds to a phase error

$$\delta\phi < (S/N)\text{-}],$$

ic. a phase error smaller than the inverse of the signal to noise ratio Consequently to fully utilize a spectrum with a signal to noise ratio of 10^3, the phase error must be less than 10^{-3} radians or 1 milliradian. This condition may be inverted to specify the signal to noise ratio necessary to obtain a reliable estimate of the phase. Increasing the discriminator reduces the number of lines used in the phase determination but improves the quality of the phase estimate and hence reduces the phase error. In the case of the Fe-Ne spectrum changing the discriminator from an intensity of $0.3I_{max}$ to $0.001I_{max}$ increases the number of lines by nearly a factor of 10, and increases the phase error by a factor of 10 as well (Table 1 and Figure 7a).

IVd. Smoothing **by** polynomial fitting

Once an accurate estimation of the phase has been obtained it is necessary to smooth this function to produce a reasonable phase spectrum for all wavenumbers within the spectral window. The usc of a least square fit to a polynomial has no practical justification other than convenience, and the accuracy of the fit relative to the order of the polynomial will reflect the complexity of the phase spectrum. Within the limits of the data a phase fit with a fcw terms suffices to describe the data, and the differences between the curves for three and eight terms arc virtually indistinguishable. Outside the data window the fits diverge rapidly, especially for higher order polynomials. Quantitative phase error can only be determined by calculating the phase error for various order polynomials: as demonstrated in Table 2 and Figure 7b, accurate fitting of the phase requires more than 4 terms, but more than seven terms does not improve the phase fit,

IVe. Results and improved wavenumber calibration

The phase difference between the low resolution phase spectrum and the least-square phase spectrum (Figure 8) matches the wavenumber differences given in Figure 4, confirming the suspicion that the wavenumber differences between the two FTS spectra arose from a phase error in onc of the spectra. The relative scale between the two graphs is consistent with the expression

$$\delta\sigma_{phase} = \frac{W\delta\phi}{2} \tag{15}$$

for lines with widths on the order of 0.1 cm-1 (100 milliKayser). Phase correction with the least-square phase spectrum leads to an improved calibration of the two FTS spectra, as illustrated in Figure 9: the wavenumber differences cluster in two groups indicating some residual phase discrepancy between the two data sets; however at this level the error has an insignificant effect for spectra with signal to noise ratios below 104.

V. Internal Calibration: the Ritz Test

The above discussion focuses on the analysis of several overlapping spectra and through the process of intercomparison it was possible to determine that at least onc of the spectra produced inconsistent results. A test that could compare various lines within a single spectrum would allow for direct determination of the phase error without requiring comparison with other similar spectra. The Ritz combination principle can be applied to a single spectrum to dctcrminc energy levels, and by considering several transitions that connect the same upper and lower states through different intermediate states it is possible to compare lines from different spectral regions within onc spectrum. If the phase error is negligible then the difference between the two different transition pathes (A+B) and (C+D) should not be a function of onc of the intermediate transition frequencies (line D for example in Figure 10). In contrast, the dependance of the difference on line frequency illustrated in Figure 11, is direct evidence that there is some distortion of the line positions in the spectrum. Hindsight, and the relative

similarity of the wavenumber differences and phase error displayed in Figures 4 and 8, suggest that the line position distortion results directly from the phase error created by the usc of a low resolution phase correction method.

Traditionally, the Ritz test has been used to verify the consistency of energy level assignments in molecular and atomic spectroscopy. In the case of an analyzed spectrum (such as Fe I), the Ritz test can, instead, bc used to verify the internal consistency of the data.

VI. Conclusions

The process of phase correcting Fourier transform emission spectra has been reexamined and a ncw method is proposed and evaluated, The traditional method of determining the phase from a symmetric low resolution portion of the spectrum is expanded into three steps: phase measurement from an intermediate resolution symmetric portion of the interferogram, phase discrimination based on signal-to-noise considerations in the amplitude spectrum, and phase smoothing using least square fitting to a polynomial expression. The effect of this method of phase determination is evaluated by comparing several transforms of overlapping spectra, and the dependance on resolution in the phase determination, discriminator, and order of polynomial arc evaluated numerically. The improvement in wavenumber calibration between overlapping spectra is very significant and represents an important step in obtaining consistent and reproducible secondary standard line positions,

VII. Acknowledgements

M.C.A. gratefully acknowledges the support of Imperial College and Chelsea instruments during a postdoctoral visit. The work described in this paper was performed at Blackett Laboratory, Imperial College, Publication support was provided by the Jet Propulsion Laboratory, California Institute of Technology, under a contract with the National Aeronautics and Space Administration. The spectra were obtained at the National Solar Observatory , National Optical Astronomy Observatory, Tucson, Arizona, which is operated by the Association of Universities for Research in Astronomy, Inc., under contract with the National Science Foundation. The generous technical support of the Kitt Peak National Solar Observatory staff is also acknowledged, particularly Greg Ladd.

Vi] I. References

[1] Brault, J. W., High Precision Fourier Transform Spectrometry: The Critical Role of Phase Correct ions, *Mikrochimica Acta [Wien]*, III ,*215,* 1987.

IX. Table List and Figure Captions

1. Table 1. RMS phase error vs. discriminator
2. Table 2, RMS Phase Error vs. Polynomial Order
3. Figure 1. An example of an unequal-sided interferogram and the apodisation function used to partition the spectrum into real and imaginary components: the resulting instrumental line shape will have a symmetric sine function real part and an antisymmetric cosine function imaginary part.
4. Figure 2. Construction of the real and imaginary components of the instrumental line shape function for a one-sided interferogram recorded with a Fourier transform spectrometer: each plot is a three dimensional representation of a complex function in either the spectral or interferogram domain (note the divergence of the tick marks and the axes is a result of the perspective used by the plotting package). (a) Symmetric component of interferogram apodisation function, (b) real, even instrumental line shape function (Fourier transform of (a), (c) antisymmetric component of interferogram apodisation function, (d) imaginary, odd instrumental line shape function (Fourier transform of (c), (c) asymmetic interferogram apodisation function (sum of (a) and (c)) for a one-sided interferogram, (f) complex instrumental line shape (Fourier transform of (c), and vector sum of(b) and (d)) – notice that if (c) is inverted, (d) is also inverted, and consequently the handedness of (f) will be reversed.
5. Figure 3. Typical low resolution (8192 points) amplitude (a) and phase (b) spectra emission spectra of a Fe-Ar hollow cathode lamp. The phase spectrum is a well defined, smooth function when the signal-to-noise ratio in the amplitude spectrum is nonzero, and in regions where the spectral intensity is low the phase determination is noisy. If the same spectra were measured with a typical number of points (128-256), then the phase spectra from the strong lines would be averaged into other regions. corrected with low resolution phase spectra.
6. Figure 4. Wavenumber differences for two overlapping spectra corrected with low resolution phase spectra.
7. Figure 5. Phase differences between phase spectrum estimates using 81920,40960,20480, and4192 samples.
8. Figure 6. Phase error at 20000 cm^{-1} as a function of apodisation width.
9. Figure 7. RMS Phase error: (a) as a function of discriminator magnitude, (b) as a function of the order of the polynomial."

10. Figure 8. The phase difference between the low resolution phase spectrum and the least-square phase spectrum.

11. Figure 9. Wavenumber differences for two overlapping spectra corrected with least squares phase spectra.

12. Figure 10. Wavenumber differences resulting from a Ritz test of several FeI lines.

Table 1: RMS **phase** error **vs.** discriminator

Discriminator Setting	*RMS Phase Error (mrad)*	*Number of Lines in Fit*
0.3	0.025	*23*
0.1	0.057	88
0.03	*0.097*	*220*
0.01	0.179	476
0.003	*0.450*	1076
0.001	0.800	2263

Table of RMS phase error as a function of **the** amplitude **of the** discriminator setting. A seven **term** least square phase polynomial was fitted for each discriminator setting.

Table 2: RMS **Phase Error vs.** Polynomial Order

Number of Terms in Polynomial	*RMS Phase Error (mrad)*
2	*57.0*
3	*20.0*
4	*3.9*
5	*1.85*
6	1,80
7	1.78
8	1.76

Table of RMS phase error versus number of **terms** in the **least** square phase polynomial with a 3% discriminator cutoff. An 80000 sample **interferogram** was transformed and 220 spectral lines were used in the **fit**.

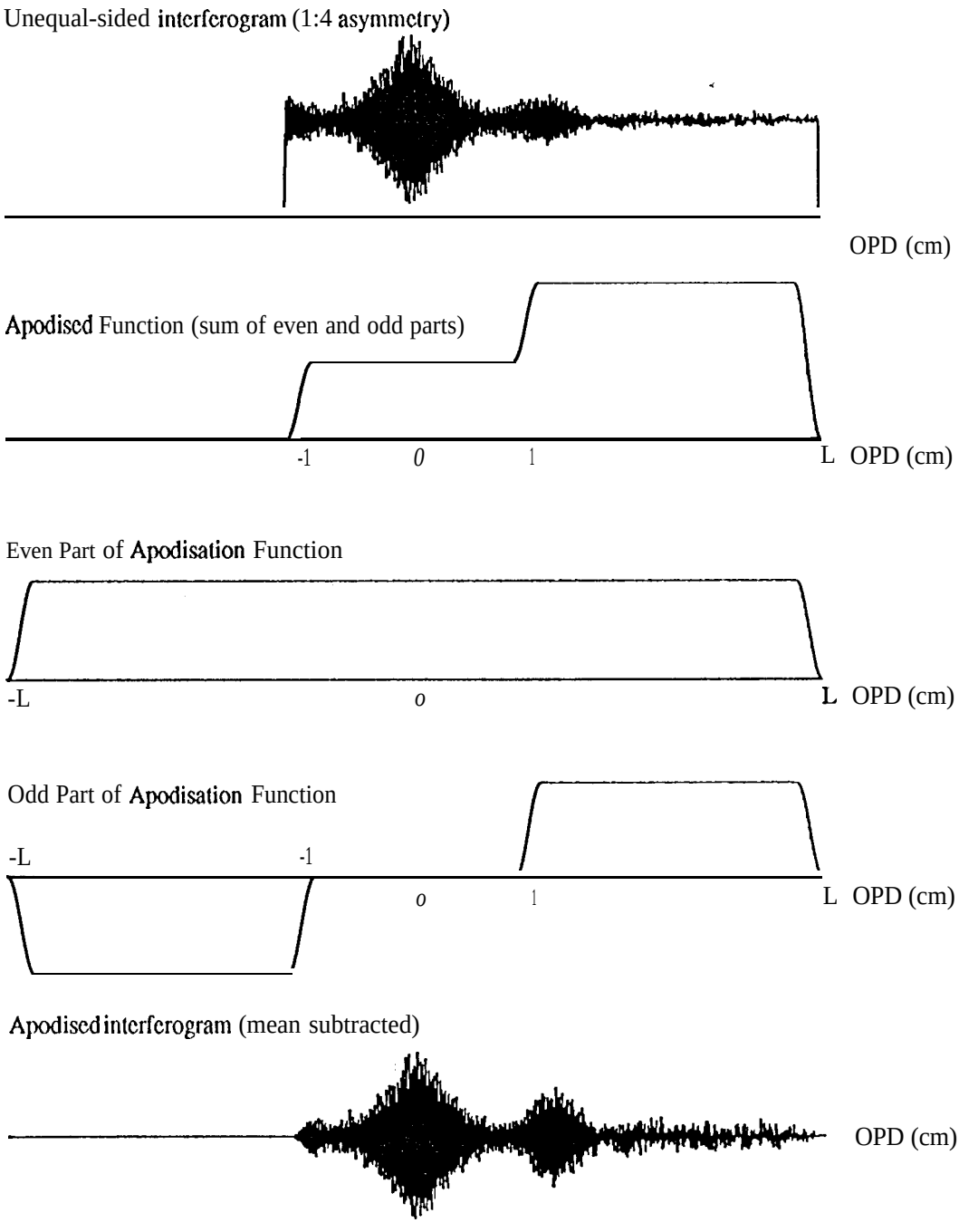

Figure J. Apodisation function and interferogram before (top) and after apodisation (bottom).

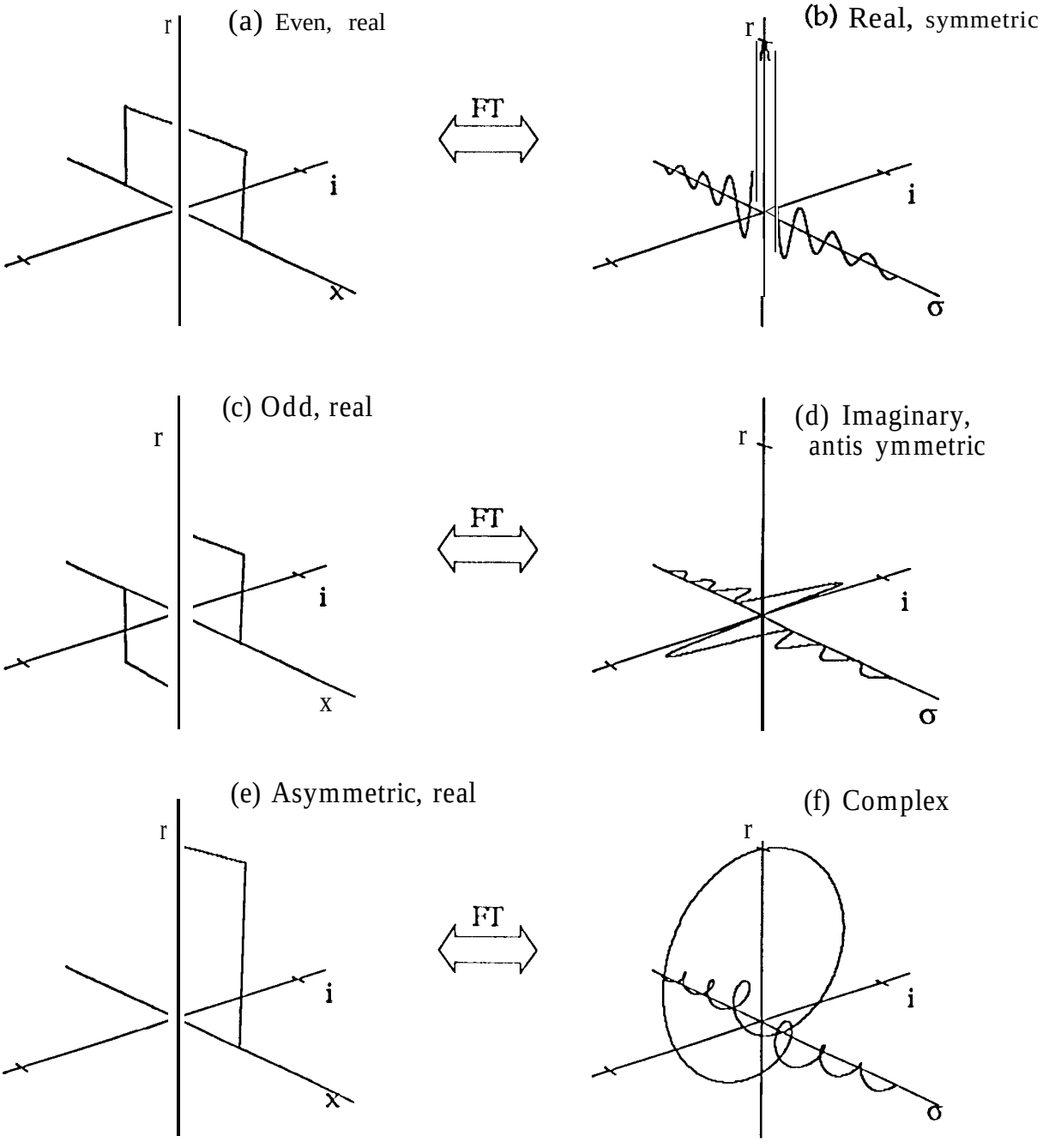
(a) Even, real
r
i
x
FT
(b) Real, symmetric
r
i
σ
(c) Odd, real
r
i
x
FT
(d) Imaginary,
antis ymmetric
r
i
σ
(e) Asymmetric, real
r
i
x
FT
(f) Complex
r
i
σ

Figure 2.

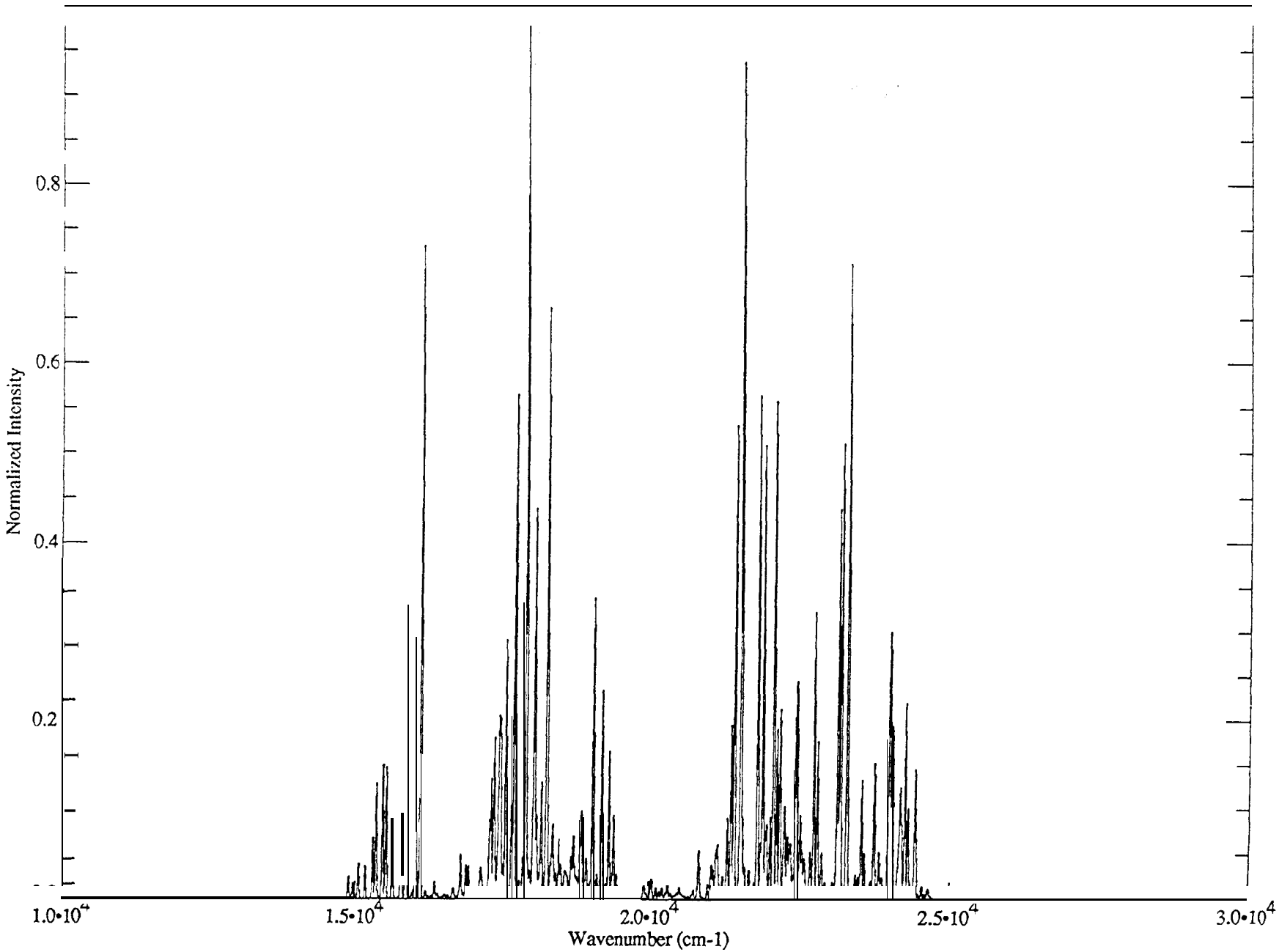
Normalized Intensity
0.8
0.6
0.4
0.2
1.0•10^4
1.5•10^4
2.0•10^4
2.5•10^4
3.0•10^4
Wavenumber (cm-1)

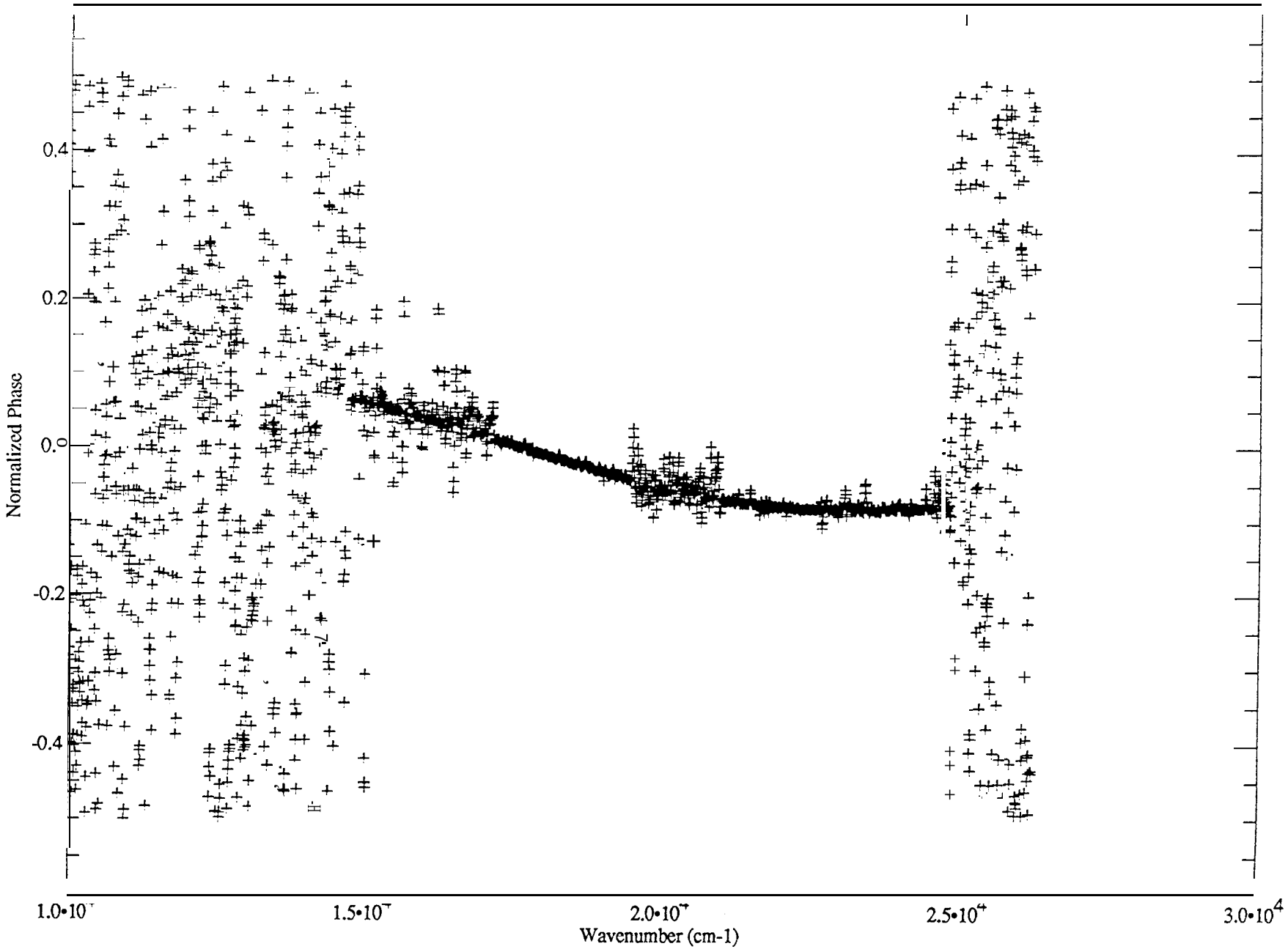
0.4
0.2
0.0
-0.2
-0.4
Normalized Phase
1.0•10⁴
1.5•10⁴
2.0•10⁴
2.5•10⁴
3.0•10⁴
Wavenumber (cm-1)

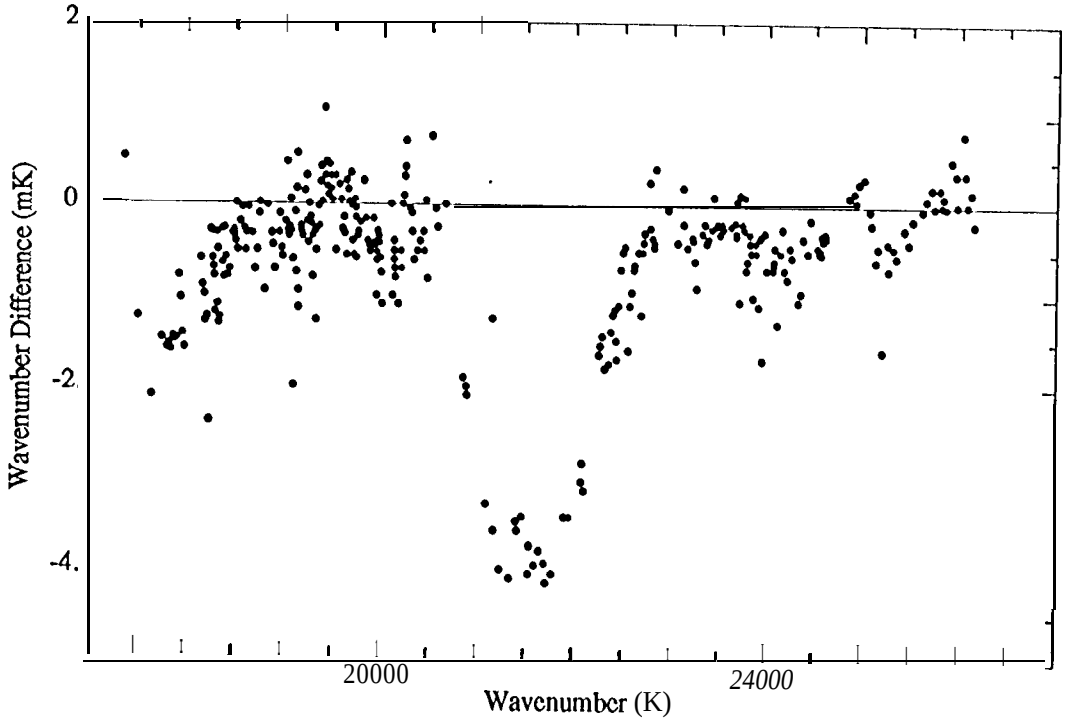

Figure 4. Wavenumber differences for two overlapping spectra correctedwith low

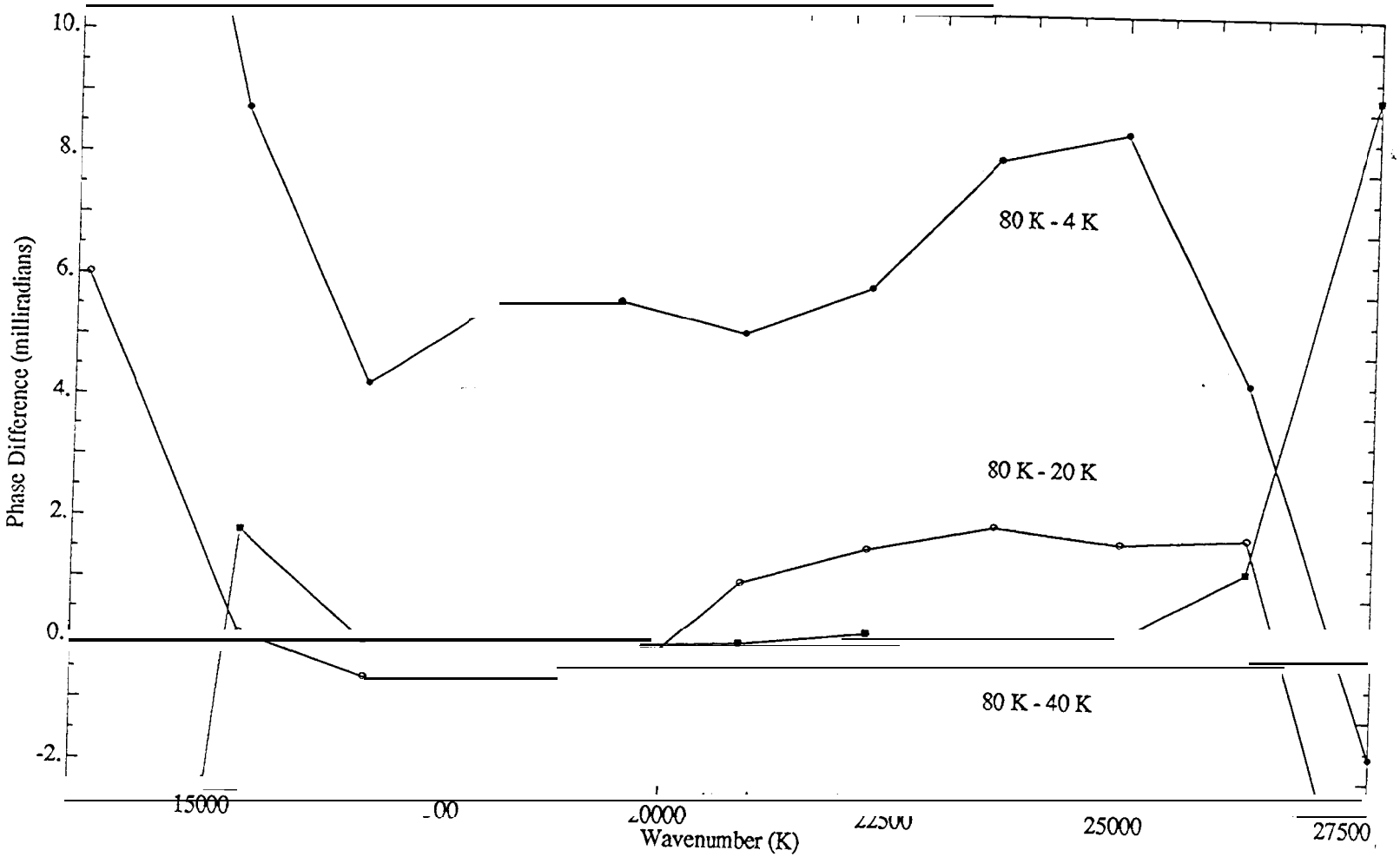

Figure 5. Phase differences between phase spectrum estimates.

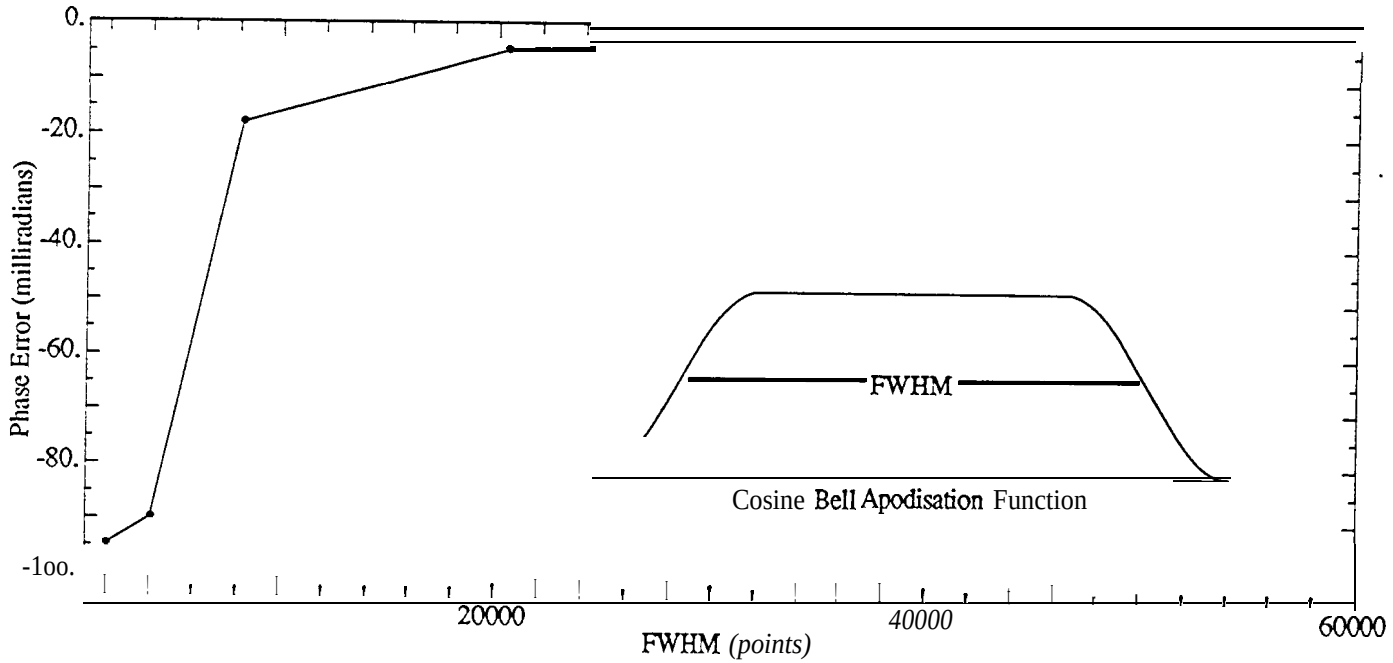

Figure 6. Phase error at 20000 cm"* as a function of apodisation width.

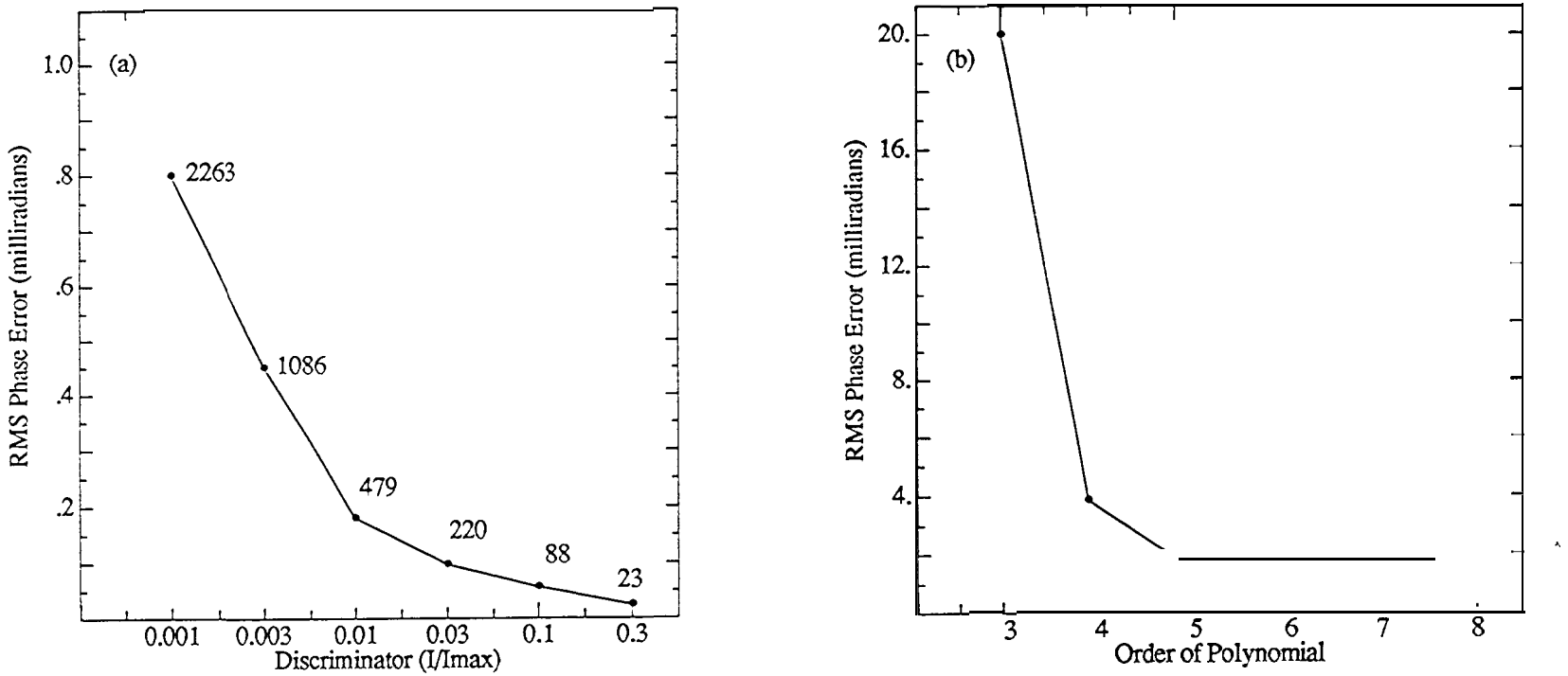

Figure 7. RMS phase error: (a) as a function of discriminator magnitude, (b) as a function of the order of the polynomial.

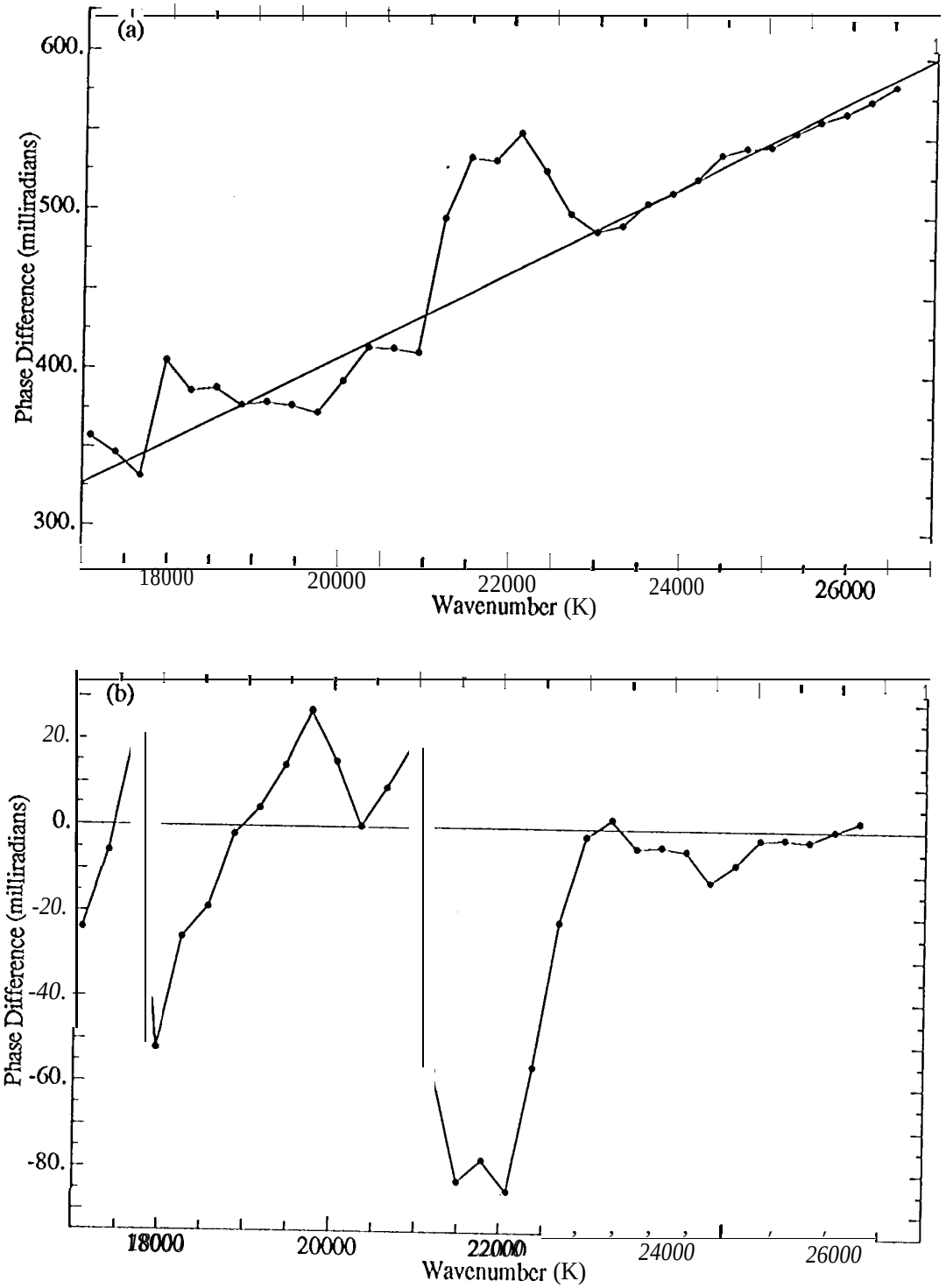

Figure 8. The phase difference between the low resolution phase spectrum and the least-square phase spectrum: (a) actual, (b) with straight line in (a) subtracted out.

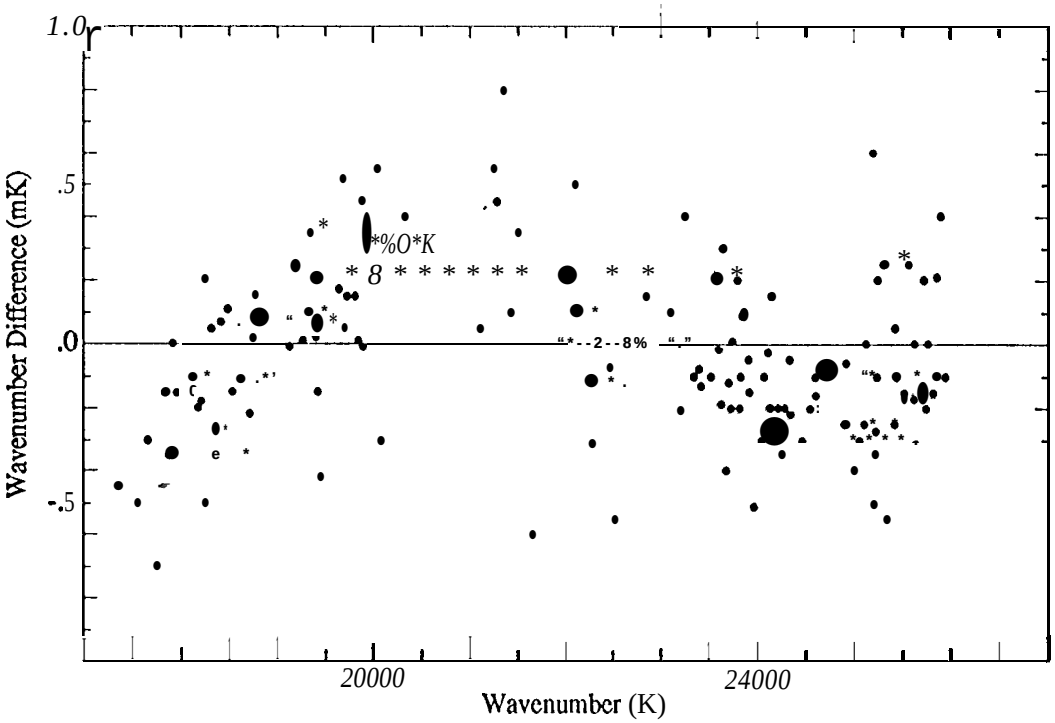

Figure 9. Wavenumber differences for two overlapping spectra corrected with least square phase spectra.

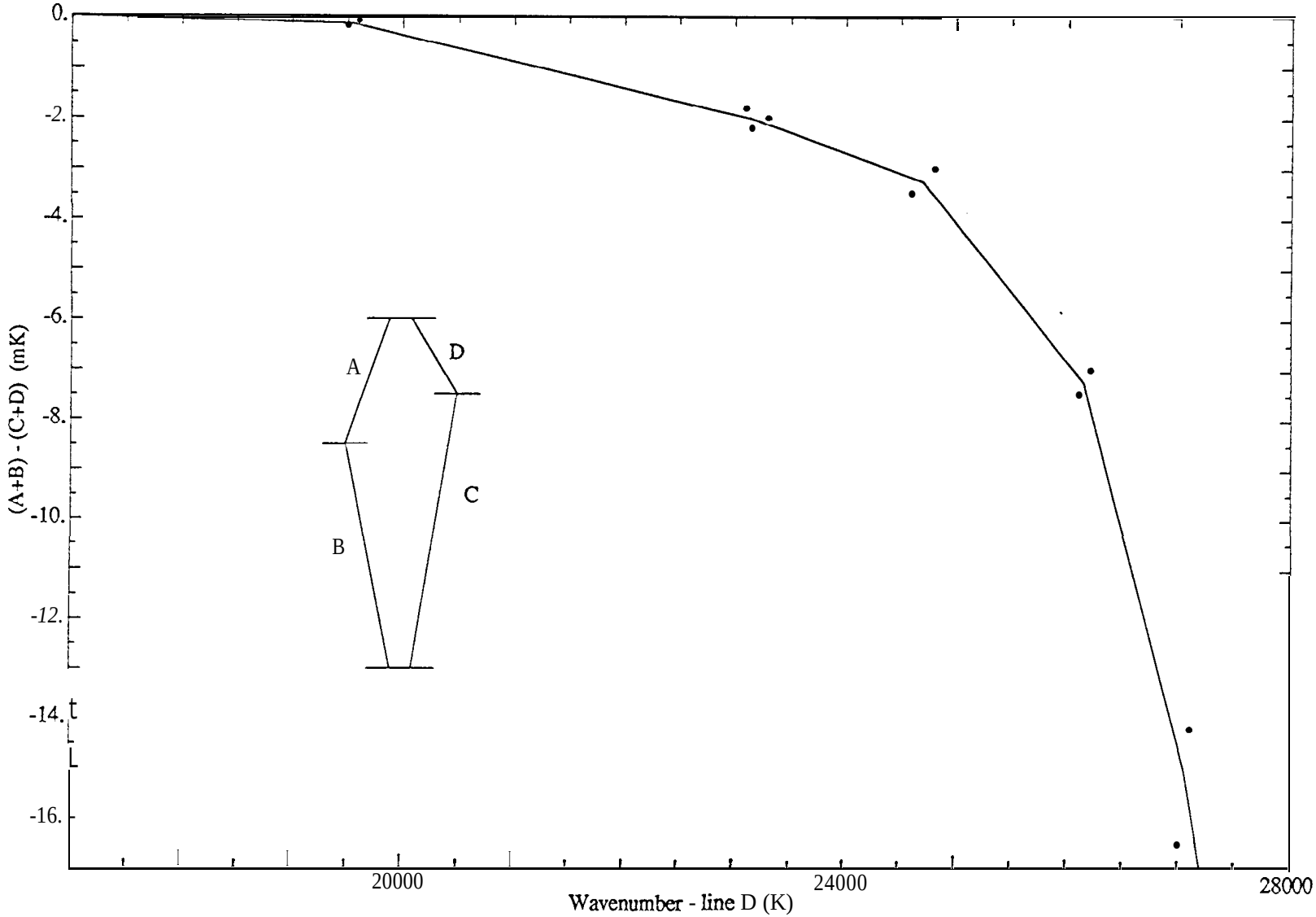

Figure 10. Wavenumber differences resulting from a Ritz test of several FeI lines.